# Magnetic catalysis and axionic charge density wave in Weyl semimetals

Bitan Roy* and Jay D. Sau

*Condensed Matter Theory Center, Department of Physics, University of Maryland, College Park, Maryland 20742, USA*

(Received 29 July 2014; revised manuscript received 22 November 2014; published 22 September 2015)

Three-dimensional Weyl and Dirac semimetals can support a chiral-symmetry-breaking, fully gapped, charge-density-wave order even for sufficiently weak repulsive electron-electron interactions, when placed in strong magnetic fields. In the former systems, due to the natural momentum space separation of Weyl nodes the ordered phase lacks the translational symmetry and represents an *axionic* phase of matter, while that in a Dirac semimetal (neglecting the Zeeman coupling) is only a trivial insulator. We present the scaling of this spectral gap for a wide range of subcritical (weak) interactions as well as that of the diamagnetic susceptibility with the magnetic field. A similar mechanism for charge-density-wave ordering at weak coupling is shown to be operative in double- and triple-Weyl semimetals, where the dispersion is linear (quadratic and cubic, respectively) for the $z$ (planar) component(s) of the momentum. We here also address the competition between the charge-density-wave and a spin-density-wave orders, both of which breaks the chiral symmetry and leads to gapped spectrum, and show that at least in the weak coupling regime the former is energetically favored. The anomalous surface Hall conductivity, role of topological defects such as axion strings, existence of one-dimensional gapless dispersive modes along the core of such defects, and anomaly cancellation through the Callan-Harvey mechanism are discussed.

DOI: 10.1103/PhysRevB.92.125141 PACS number(s): 71.55.Ak, 11.10.Jj, 14.80.Va

## I. INTRODUCTION

Three-dimensional Weyl semimetals (WSMs) represent topologically nontrivial gapless systems that support linearly dispersing quasiparticle excitations with opposite chiralities in the vicinity of two so-called Weyl points that are separated in the momentum space [1]. If Weyl fermions choose to reside at the same point in the Brillouin zone (BZ), which can occur at the transition point between the strong $Z_2$ topological and the trivial band insulators [2–8], the configuration is dubbed a Dirac semimetal (DSM). Due to momentum-space separation of Weyl nodes, the time reversal and/or the inversion (parity) symmetry is broken in WSMs, which can then lead to peculiar electrodynamic responses, such as the chiral-magnetic effect and anomalous Hall conductivity [9–18].

Similarly to monolayer graphene, three-dimensional WSMs or DSMs are also extremely robust against weak electron-electron interactions, due to the vanishing density of states [$D(E) \sim E^2$] near the apex of conical dispersions [19]. Nevertheless, if interactions are sufficiently strong, they can undergo continuous phase transitions and enter into fully gapped massive phases [20,21]. The requisite interaction strength for such instabilities may be too high to realize any ordering in the pristine system. However, the application of strong magnetic fields can trigger the ordering tendencies even for weak interactions.

Placed in a magnetic field ($B$), the linear dispersion in a WSM or DSM quenches into a set of Landau levels (LLs), and in particular, the zeroth LLs (ZLLs) for the left and right chiral fermions are composed of nondegenerate and spin-polarized one-dimensional dispersive modes with energies $\pm v k_z$, respectively, where $v$ is the quasiparticle Fermi velocity along the $z$ direction. For the sake of simplicity, we here assume the spectrum to be isotropic. Therefore, weak enough electron-electron interaction can *hybridize* the one-dimensional chiral ZLLs and develop a chiral-symmetry-breaking (CSB) spectral gap at the Weyl points [22,23]. A similar instability may also occur within the ZLL of three-dimensional nonrelativistic Fermi liquids, when placed in strong magnetic fields [24]. Due to the momentum-space separation of Weyl nodes, the CSB mass breaks the translational symmetry and represents a *charge-density-wave* (CDW) order [11,25]. The CDW order in WSMs stands as an example of the *axionic* state of matter that supports a dynamic magnetoelectric effect, captured by the $\mathbf{E} \cdot \mathbf{B}$ term, and its coefficient is tied to the separation of Weyl points [25]. The accompanying massless Goldstone mode or the *sliding* mode in the CDW phase is known as the *axion*. On the other hand, in DSMs the CSB order corresponds to a trivial insulator (neglecting the Zeeman coupling) since the Dirac points reside at the same point in the BZ.

We also address the competition between the axionic CDW order and a spin-density-wave (SDW) order. Both of them can lead to a spectral gap within the ZLL. We show that while the CDW order pushes down all filled LLs (placed below the chemical potential), the SDW order causes spin-splitting of filled LLs. Thus we believe (at least for sufficiently weak interactions) that the CDW order is energetically favored over the SDW order.

A three dimensional trivial DSM can be realized at the quantum critical point between the topological and trivial insulators (in class AII). Recent times have also witnessed the discovery of topological DSMs (two copies of superimposed WSMs protected by time-reversal, inversion, and fourfold rotational symmetries [26]) in $Cd_3As_2$ [27] and $Na_3Bi$ [28]. In the presence of magnetic fields, Zeeman coupling can separate the Weyl nodes in trivial and topological DSMs and support a WSM [29]. Various other proposals for realizing WSMs in condensed matter systems include 227 pyrochlore iridates with all in-all out antiferromagnetic ordering [30], multilayer configuration of topological and normal insulators [10,12], and magnetically doped topological insulators [31,32]. But their experimental realization remains elusive. Rather, in the recent past material realization of WSMs

*broy@umd.edu

 

has been confirmed in inversion-asymmetric TaAs [33–35], NbAs [36], and TaP [37] and time-reversal-symmetry-breaking $YbMnBi_2$ [38] and $Sr_{1-y}MnSb_2$ [39]. Therefore, the proposed many-body axionic ground state can possibly be observed in these materials in the near-future when these systems are placed in strong magnetic field. We here present the scaling behavior of this order for a wide range of subcritical interactions with the magnetic field. Formation of a spectral gap at Weyl points can lead to measurable consequences in various physical quantities and here we address its impact on the diamagnetic susceptibility (DMS). Since WSMs live at the *upper critical dimensions* ($d_{\rm up} = 3$), the scaling of the mass gap and the DMS display *logarithmic* corrections as $B \to 0$.

Our proposed mechanism for the generation of axionic CDW order at weak coupling in the presence of a strong magnetic field remains operative among the other members of the Weyl family, such as the double-WSMs and the triple-WSMs. Respectively, these two systems support two- and three-fold degenerate, spin-polarized chiral ZLLs. Thus sufficiently weak interactions can hybridize them and give rise to a CDW order. We expect that such a broken-symmetry phase can be realized in various double-WSMs, such as $HgCr_2Se_4$ [40–42] and $SrSi_2$ [43]. Our conclusion regarding the competition between the CDW and the SDW orders in regular WSMs remains unaltered for these two systems as well.

In this work we also address the correction to anomalous transport properties in various members of the Weyl family in the presence of an underlying axionic CDW order. In the uniform phase, the axionic CDW order gives rise to anomalous charge transport on the surface, which receives contributions from the one-dimensional chiral surface states as well as from bulk scattered states, the gapped ZLLs. In the ordered phase the axionic CDW can also accommodate topological defects, such as line vortices, known as *axion strings*. We here show that such a topological defect hosts a gapless one-dimensional dispersive mode in its core. Such a gapless mode carries a dissipationless current, which in turn is supplied radially from the bulk, according to the Callan-Harvey mechanism. The number of one-dimensional gapless mode is shown to be proportional to the topological invariant of the system.

The rest of the paper is organized as follows. In the next section, we derive the LL spectrum in WSMs and discuss the possibility of realizing various broken-symmetry phases and the competition between the CDW and the SDW orders at weak coupling. Section III addresses the change renormalization and DMS in the presence of a spontaneously generated spectral gap at the Weyl nodes. In Sec. IV, we analyze the scaling behavior of the spectral gap and compare our results with a recent experiment. Generalization of the magnetic catalysis mechanism for the other members of the Weyl family (such as double- and triple-WSMs) is discussed in Sec. V. Discussions on the chiral anomaly, anomalous transport, the role of topological defects, and the Callan-Hervey mechanism in the axionic CDW phase are presented in Sec. VI. We summarize our findings in Sec. VII. The derivation of the gap equation in the presence of a magnetic field is relegated to the Appendix.

## II. LANDAU LEVELS AND MAGNETIC CATALYSIS

We begin the discussion by computing the LL spectrum in WSMs. Let us define a four-component spinor $\Psi^\top(\vec{k}) = [\Psi_L(\vec{k}), \Psi_R(\vec{k})]$, where $\Psi_X(\vec{k})$ are two-component spinors, organized as $\Psi_X^\top(\vec{k}) = [\Psi_{X,\uparrow}(\pm\vec{Q}+\vec{k}), \Psi_{X,\downarrow}(\pm\vec{Q}+\vec{k})]$ for $X = L, R$. Weyl nodes are located at $\pm\vec{Q}$, where nondegenerate, linearly dispersing left (L) and right (R) chiral bands cross zero energy, respectively, and $\uparrow$ and $\downarrow$ are the Kramers partners or two spin projections. For the sake of simplicity, we choose $\vec{Q} = Q\hat{z}$, whereas in pristine DSMs $|\vec{Q}| = 0$. The response of these systems to electromagnetic fields ($\vec{A}$) is captured by the Hamiltonian

$$H[\vec{A},\vec{a}] = \sum_{j=1}^{3} i\gamma_0\gamma_j(v\hat{k}_j - eA_j - \tilde{g}\, a_j\gamma_5) \qquad (1)$$

in the low-energy limit, where $e$ is the electronic charge. Mutually anticommuting $\gamma$ matrices are $\gamma_0 = \tau_1 \otimes \sigma_0$, $\gamma_5 = \tau_3 \otimes \sigma_0$, and $\gamma_j = \tau_2 \otimes \sigma_j$ for $j = 1$, 2, and 3, respectively. $\tau_0$ ($\sigma_0$) and $\tau_j$ ($\sigma_j$) are, respectively, the two-dimensional identity and standard Pauli matrices, operating on the chiral (spin) index. The external magnetic field $\vec{B}(=\vec{\nabla}\times\vec{A}) = B\hat{z}$ is set to be along the $z$ direction. In Eq. (1), we have allowed the axial vector potential $a_3 = B$, which supports Weyl points at $\pm\vec{Q}_Z$, where $\vec{Q}_Z = \tilde{g}B\hat{z}$ (say) [29,45]. For example, at the quantum critical point between topological and trivial insulators massless Dirac fermions are realized at the $\vec{k} = (0,0,0)$ point and application of a magnetic field gives rise to Weyl points at $\pm\vec{Q}_Z$. The explicit dependence on the axial vector potential from Eq. (1) can, however, be eliminated by setting $\vec{Q} = \vec{Q}_Z$ in the spinor definition of $\Psi(\vec{k})$.

The orbital coupling of the uniform magnetic field supports a set of LLs at energies $\pm\sqrt{2nB + v^2k_z^2}$ [setting $a_j = 0$ in Eq. (1)] for $n = 0,1,\ldots$, with degeneracy per unit area $\frac{2-\delta_{n,0}}{2\pi l_B^2}$, where $l_B \sim \frac{1}{\sqrt{eB}}$ is the magnetic length in WSMs. The spin-polarized ZLL contains two branches of one-dimensional dispersive modes with energies $\pm vk_z$. The ZLLs are eigenstates of $\gamma_5$, the generator of *chirality*, with eigenvalues $\pm 1$. In the continuum description $\gamma_5$ is also the generator of U(1) translational symmetry in WSMs and $[H[\vec{A},\vec{a}],\gamma_5] = 0$. An infinitesimal interaction can, therefore, hybridize the left and the right chiral ZLLs and develop a mass gap at the Weyl points through a BCS-like mechanism (due to the effective dimensional reduction of the system in the magnetic field). This mechanism is also known as *magnetic catalysis* [22,23].

To gain insight into the nature of the CSB order, we consider a generic effective single-particle Hamiltonian,

$$H[\vec{m},\vec{n},Q_3] = H[\vec{A},0] + m_1\gamma_0 + m_2 i\gamma_0\gamma_5 + n_1\gamma_3 + n_2 i\gamma_5\gamma_3 + Q_3 i\gamma_0\gamma_3\gamma_5, \qquad (2)$$

where $\vec{m} = (m_1,m_2) = |\Delta|(\cos\phi, \sin\phi)$ is the complex CDW order parameter, and $\phi$ is the associated U(1) angle. Eigenvalues of $H[\vec{m},0,0]$ are $\pm\sqrt{2nB + v^2k_z^2 + |\Delta|^2}$ for $n = 0,1,\ldots$. Therefore, $\Delta$ introduces a spectral gap within the ZLL ($n = 0$) and, in addition, pushes all the filled LLs ($n \geqslant 1$) at negative energies farther down. Hence, formation of Dirac masses within the ZLL is energetically quite favored.

In WSMs nondegenerate left and right chiral fermionic excitations live around $\pm\vec{Q}$, hence

$$\Delta \sim \exp(-2i\ \vec{Q}\cdot\vec{r})\ \langle c_{\vec{Q}}^\dagger\ c_{-\vec{Q}}\rangle$$

represents a translational-symmetry-breaking CDW order, with periodicity $2\vec{Q}$. Breaking of translational symmetry can be appreciated from the anticommutation relation among two mass matrices appearing in Eq. (2) and the generator of translation $\{\gamma_0,\gamma_5\} = \{i\gamma_0\gamma_5,\gamma_5\} = 0$. Such translational-symmetry-breaking order can arise from the four-fermion interaction

$$H_{\rm int}^{\rm CDW} = g[(\Psi^\dagger\gamma_0\Psi)^2 + (\Psi^\dagger i\gamma_0\gamma_5\Psi)^2], \tag{3}$$

which corresponds to the celebrated Nambu-Jona-Lasinio model for mass generation of relativistic fermions through spontaneous chiral symmetry breaking [44].

Next we discuss the effect of the terms proportional to $n_1,n_2$ in Eq. (2). The spectrum in the effective Hamiltonian $H[0,\vec{n},0]$ is given by $\pm\sqrt{(\sqrt{2nB}+\sigma N)^2 + v^2k_z^2}$ for $\sigma = \pm$, where $N = \sqrt{n_1^2+n_2^2}$. Degeneracy of the LLs is $\frac{1}{2\pi l_B^2}$ for $n = 0,1,\ldots$. The four-fermion interaction that can support such a SDW order is

$$H_{\rm int}^{\rm SDW} = g'[(\Psi^\dagger\gamma_3\Psi)^2 + (\Psi^\dagger i\gamma_3\gamma_5\Psi)^2]. \tag{4}$$

The fermionic bilinears $\langle\Psi^\dagger\gamma_3\Psi\rangle = n_1$ and $\langle\Psi^\dagger i\gamma_5\gamma_3\Psi\rangle = n_2$ represent two components of a translational-symmetry-breaking SDW order with periodicity $2\vec{Q}$, which gaps out the ZLL ($n = 0$) but splits the filled LLs, placed below the chemical potential. Therefore, the SDW order, although introduces a spectral gap within the ZLL, is expected to be energetically inferior to the CDW order, which, besides gapping the ZLL out, also pushes down the filled LLs. Therefore, we strongly believe that the CDW is the natural ground state in WSMs, when they are placed in a strong magnetic field, at least for weak repulsive interactions. Thus, from now on we focus on the CDW order.

In Eq. (2) we have also allowed a term ($\sim Q_3$) that can be dynamically generated by electronic interactions and renormalize the location of Weyl points [45]. Following the same procedure described above, $Q_3$ can be eliminated from Eq. (2) by taking $Q\hat{z} \to (Q+Q_3)\hat{z}$ in the definition of spinor $\Psi(\vec{k})$. However, a finite $Q_3$ modifies the periodicity of CDW order to $2(Q+Q_3)\hat{z}$ [46]. The four-fermion interaction $g_5(\Psi^\dagger i\gamma_0\gamma_3\gamma_5\Psi)^2$ can, in principle, renormalize the location of the Weyl nodes, where $Q_3 \sim g_5(l_B)\langle\Psi^\dagger i\gamma_0\gamma_3\gamma_5\Psi\rangle$, and $g_5(l_B)$ is the strength of the four-fermion interaction $g_5$ at the scale $l_B$.

Formation of the CDW order can also occur when the system is placed slightly away from the charge-neutrality point. CDW order with periodicity $2|Q+\frac{|\mu|}{v}|$ develops in WSMs at finite chemical doping ($\mu$), at least when $|\mu| < \sqrt{2B}$. In $Cd_3As_2$ and $Na_3Bi$ the field-induced (by Zeeman coupling) Weyl nodes are located at $(\pm Q_0 \pm Q_z)\hat{z}$ [47]. Hence, the periodicity of field-induced CDW order in these topological DSMs is $2|Q_z|$ (assuming that the periodicity of the CDW order is unique), which can be measured by scanning tunneling microscopy, for example. If we completely neglect the Zeeman coupling and set $Q_3 = 0$ in DSM, one enjoys the liberty of setting $\phi = 0$ and $\Delta(=m_1)$ then represents a trivial Dirac mass. However, the scaling of DMS ($\chi$) and mass gap ($\Delta$) is insensitive to the exact nature of the CDW ordering, and depends only in its amplitude (at least in the mean-field limit).

## III. CHARGE RENORMALIZATION AND DIAMAGNETIC SUSCEPTIBILITY

We now analyze the effects of mass generation near the Weyl points in the presence of magnetic fields on DMS, and the renormalization of the electric charge and the magnetic field. In magnetic fields, the free energy density ($F$) of the system scales as $F \sim \sqrt{eB}/l_B^3$, where $\sqrt{eB}$ is the LL energy, and thus $F \sim (eB)^2$. Hence, a naive scaling argument indicates a *constant* DMS ($\chi$) in WSMs. However, the free energy and DMS receive logarithmic corrections, since the system lives at the upper critical dimension, which we capture pursuing a field theoretic approach [48,49]. For simplicity, we consider a constant CSB mass ($\Delta$). The DMS then acquires contribution only from the higher LLs ($n \geqslant 1$) and the free energy is given by

$$\begin{aligned} F &= \left(-\frac{1}{\pi l_B^2}\right)\times\int_{-\infty}^{\infty}\frac{dk_z}{2\pi}\sum_{n=1}^{\infty}\sqrt{v^2k_z^2+\Delta^2+n\frac{2v^2}{l_B^2}} = \left(-\frac{v}{\pi l_B^2}\right)\times\lim_{\epsilon\to 0}\int_{-\infty}^{\infty}\frac{dk_z}{2\pi}\sum_{n=1}^{\infty}\left[\frac{2}{l_B^2\Lambda^2}\left[\frac{k_z^2l_B^2}{2}+\frac{\Delta^2l_B^2}{2v^2}+n\right]\right]^{\frac{1}{2}-\frac{\epsilon}{2}} \\ &= \left(-\frac{v^2}{2\pi^2l_B^4}\right)\times\left[\frac{2H\zeta\left(-1,1+\Delta_R^2\right)}{\epsilon}+\left\{\log\left(\frac{\Lambda^2l_B^2}{2}\right)+0.386\right\}\times H\zeta\left(-1,1+\Delta_R^2\right)+H\zeta'\left(-1,1+\Delta_R^2\right)\right] \\ &= \left(\frac{v^2}{24\pi^2l_B^4}\right)\times\left(\frac{2}{\epsilon}F_1(\Delta_R)+\left[\log\left(\frac{\Lambda^2l_B^2}{2}\right)+0.386\right]F_1(\Delta_R)-F_1'(\Delta_R)\right), \end{aligned} \tag{5}$$

where $\Lambda$ is the ultraviolet (UV) cutoff for the conical dispersion in WSM, $\Delta_R = \frac{\Delta l_B}{\sqrt{2}v}$, and $H\zeta$ is the Hurwitz zeta function. The function

$$F_1(x) = -12H\zeta[-1,1+x^2] \tag{6}$$

with $F_1(0) = 1$ and its scaling is shown in Fig. 1. The term proportional to $\frac{1}{\epsilon}$ can be identified as the logarithmically divergent part of the free energy, which can be removed through the renormalization of the electric charge ($e$) and magnetic field ($B$) according to

$$e_R^2 = e^2\left[1-\frac{e^2v}{12\pi^2}F_1(\Delta_R)\times\frac{1}{\epsilon}\right], \tag{7}$$

$$B_R^2 = B^2\left[1+\frac{e^2v}{12\pi^2}F_1(\Delta_R)\times\frac{1}{\epsilon}\right], \tag{8}$$

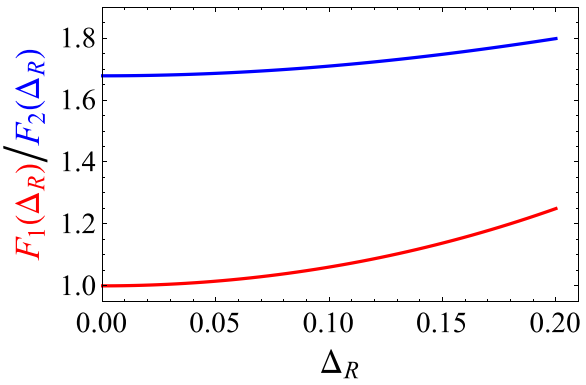


FIG. 1. (Color online) Scaling of two functions $F_1$ and $F_2$, appearing in the expression of DMS [see Eq. (9)], with $\Delta_R$.

where quantities with subscript $R$ represent their renormalized values. The logarithmic correction in the free energy at $T = 0$ is determined by the largest energy scale among $\sqrt{eB}$ and $\Delta$, which sets the infrared cutoff of the theory. For weak interactions $\sqrt{eB} \gg \Delta$, and the logarithmic correction is given by $\log(B_0/B)$, where $B_0 \sim \Lambda^2$ is the magnetic field associated with the lattice spacing.

The finite part of the free energy gives DMS

$$\chi = \left(-\frac{e_R^2 v}{24\pi^2}\right)\left[F_1(\Delta_R)\log\left(\frac{B_0}{B}\right) + F_2(\Delta_R)\right], \quad (9)$$

where the function

$$F_2(x) = 12[0.31H\zeta[-1,1+x^2] - H\zeta'(-1,1+x^2)]. \quad (10)$$

Scaling of $F_2(x)$ is shown in Fig. 1 and $F_2(0) = 1.68$. Therefore, DMS in WSMs, in addition to a constant value, also manifests a *logarithmic* enhancement as $B \to 0$, which can be measured in the small-field limit. Equation (9) suggests that DMS, besides the logarithmic correction, also acquires nontrivial contributions due to the gap generation in the magnetic field (see Fig. 1). We expect such corrections to DMS can be observed in experiments.

## IV. SCALING OF THE SPECTRAL GAP

In the previous section, we assumed that the spectral gap at the Weyl point is insensitive to the strength of the magnetic field. However, the CSB mass displays a nontrivial dependence on the magnetic field and the interaction strength, which we explore in this section. The qualitative behavior of DMS remains the same, even when $\Delta = \Delta(B)$.

The condensation energy in the presence of CSB order is

$$E = \frac{\Delta^2}{4g} - \int_{-\infty}^{\infty}\frac{dk_z}{2\pi}\sum_{n=0}^{\infty}(2-\delta_{n,0})\frac{\sqrt{2nB + v^2k_z^2 + \Delta^2}}{2\pi l_B^2}. \quad (11)$$

We consider here only the short-range component ($g$) of the Coulomb interaction that supports the CSB order. Minimizing $E$ with respect to $\Delta$, we obtain the gap equation [50]

$$\frac{1}{g} = B\int_{\Lambda^{-2}}^{\infty}\frac{ds}{s}e^{-s\Delta^2}\coth(sB), \quad (12)$$

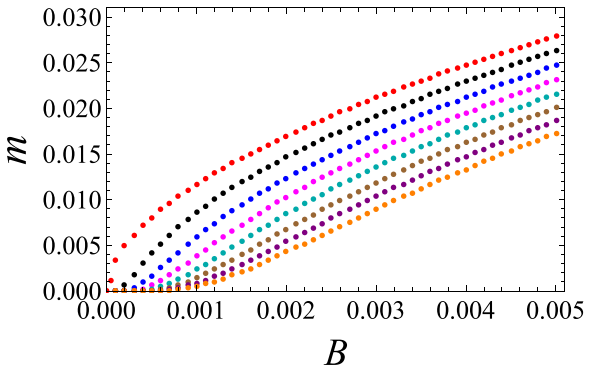


FIG. 2. (Color online) Scaling of CSB mass ($m$) with magnetic field ($B$) for interaction strength, decreasing from top to bottom, parametrized by $\delta(=(g_c - g)/gg_c\Lambda^2) = 0$, 0.01, 0.02, 0.03, 0.04, 0.05, 0.06, and 0.07. Here, $m$ is measured in units of $v\Lambda$, and $B$ in units of $B_0 \sim \Lambda^2$; the magnetic field associated with the lattice spacing ($a \sim 1/\Lambda$).

after completing the integral over $k_z$ and taking $2\pi^2/g \to 1/g$. A detailed derivation of the gap equation is available in the Appendix. The right-hand side of the above equation discerns a UV divergence as we take $\Lambda \to \infty$, which can be regularized by introducing a quantity $\delta = (g\Lambda^2)^{-1} - (g_c\Lambda^2)^{-1}$ that measures the deviation from the zero-magnetic-field critical strength of the interaction ($g_c$) for CSB ordering, defined as $g_c^{-1} = \int_0^\infty dx\,K(x)/x^2$. The function $K(x)$ satisfies $K(x \to 0/\infty) = 0/1$, otherwise arbitrary. In terms of the dimensionless gap $\frac{\Delta}{v\Lambda} \to m(\ll 1)$ and magnetic field $\frac{B}{\Lambda^2} \to B(\ll 1)$, the gap equation simplifies to

$$\delta + I_1(m,B) + I_2(m,B) + \mathcal{O}(m^6, B^4, y^{-4}) = 0, \quad (13)$$

where

$$\frac{I_1(m,B)}{2B} = a - \frac{b}{y^2} + \frac{c}{y^3} - \frac{y+1}{2y}\left[\log(2B) - B + \frac{B^2}{6}\right],$$
$$\frac{I_2(m,B)}{B} = \gamma_E + 2\log(m) - m^2 + \frac{m^4}{4}, \quad (14)$$

and $y(=B/m^2) \gg 1$, for a subcritical ($g < g_c$ or $\delta > 0$) strength of the interaction. $\gamma_E$ is the Euler-Mascheroni constant, and $a = 0.63$, $b = 0.21$, $c = 0.05$ (see the Appendix). Numerical solutions of the above gap equations for a wide range of subcritical interactions are presented in Fig. 2. The mass gap acquires logarithmic corrections as $B \to 0$, since the system lives at an upper critical dimension ($d_{\rm up} = 3$).

So far we have considered only the short-range parts of the Coulomb interaction and neglected its long-range tail since dielectric constants in semiconductors are typically very high (~10–30). A weak long-range interaction is a *marginally* irrelevant perturbation in WSMs and gives rise to a logarithmic correction to the Fermi velocity ($v$) [49,51,52] according to $v \approx v_0[1 + \alpha\log(B/B_0)]$ in magnetic fields, where $v_0$ is the bare Fermi velocity and $\alpha$ is the fine-structure constant. Therefore, the mass gap ($m$) also acquires an additional logarithmic correction, since $m$ is measured here in units of $v\Lambda$ [50]. The DMS ($\chi$), quoted in Eq. (9), also receives an additional logarithmic correction from the long-range tail of the Coulomb interaction, as $\chi$ is expressed as a function of $\Delta_R = \Delta l_B/(\sqrt{2}v)$.

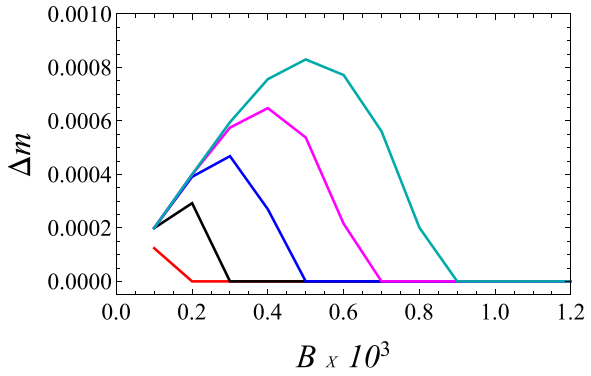


FIG. 3. (Color online) Scaling of the difference between the total gap $m_t(=m_b+m)$ and the interaction-driven gap $(m)$; $\Delta m = m_t - m$ as a function of dimensionless magnetic fields $B = B/\Lambda^2$, for $\delta = 0.01$ (red line), $\delta = 0.02$ (black line), $\delta = 0.03$ (blue line), $\delta = 0.04$ (magenta line), and $\delta = 0.05$ (cyan line).

In a recent experiment, LL quantization has been observed in $Cd_3As_2$ [53]. However, the crystal was cleaved along a low-symmetry axis (112), and consequently the underlying $C_4$ symmetry, protecting the gapless semimetallic phase [26], is lost. Therefore, even the noninteracting Hamiltonian gives rise to a gap in the spectrum, which possibly scales as $m_b = m_0 B$ (to the leading order), and $m_0$ is chosen such that at $B = 12$ T, $m_b$ produces a noninteracting gap of 1.4 meV, in qualitative agreement with Ref. [53]. Performing self-consistent calculation of the total gap $m_t = m + m_b$ we find that for weak magnetic fields the noninteracting gap $m_b$ dominates over the interaction-driven mass gap $(m)$, which overwhelms the former contribution at stronger fields. Such crossover, however, takes place at stronger magnetic fields as the interaction gets weaker, as shown in Fig. 3.

$Cd_3As_2$ and $Na_3Bi$ cleaved along the high-symmetry axis, so that the underlying $C_4$ symmetry is preserved, provides the ideal situation to observe only the interaction-induced gap at Weyl points. Alternatively, one can also compare the scaling of this gap with the magnetic field at different temperatures. At high temperatures the gap is determined by its noninteracting component $(m_b)$, which is expected to scale linearly with the magnetic field, whereas at sufficiently low temperatures the interaction-driven gap $(m)$ can take over $m_b$. The critical temperature for the CDW transition is $T_c \sim \exp(-1/[gD(B)])$, where $D(B)$ is the density of states of the ZLL (BCS scaling). Thus subtracting the $B$-linear part of the gap, obtained from its high-temperature scaling, one can extract the scaling behavior of the interaction-induced gap in magnetic fields at low temperatures $(T < T_c)$. Therefore, the CSB mechanism for insulation in WSMs can be identified from the temperature dependence of the magnetic-field-induced gap [53] and, also, from the scaling of DMS.

## V. MAGNETIC CATALYSIS IN DOUBLE- AND TRIPLE-WEYL SEMIMETALS

The magnetic catalysis for the gap formation in WSMs at weak coupling remains operative for the other members of the Weyl family, such as double- and triple-WSMs. Respectively, these two systems display quadratic and cubic dispersions in the $x$-$y$ plane and a linear dispersion along the $z$ direction in the vicinity of Weyl nodes, located at $\pm\vec{Q}$. For example, double-WSMs can be realized in $HgCr_2Se_4$ [40–42] and $SrSi_2$ [43], although the material realization of triple-WSMs remains illusive. The bulk topological invariants in double- and triple-WSMs are, respectively, twice and thrice that in WSMs, and consequently one-dimensional chiral surface states carry an additional two- and three-fold degeneracy.

The low-energy Hamiltonian in double-WSMs, placed in a magnetic field $\vec{B} = B\hat{z}$, reads as

$$H_2[\vec{A}] = i\gamma_0\left[\gamma_1\left(\frac{\pi_x^2-\pi_y^2}{2m^*}\right)+\gamma_2\left(\frac{2\pi_x\pi_y}{2m^*}\right)+\gamma_3 v k_z\right], \tag{15}$$

where $\pi_j = (-i\partial_j - A_j)$ and $m^*$ is the effective mass of the parabolic dispersion in the $x$-$y$ plane. The spectrum of LLs goes as $\pm\sqrt{n(n-1)\omega_c^2 + v^2k_z^2}$ for $n = 0,1,2,\ldots$, where $\omega_c$ is the cyclotron frequency. Therefore, double-WSMs also host one-dimensional spin-polarized chiral ZLLs, which, carry an extra twofold *orbital degeneracy* (for $n = 0,1$) [54]. Hence, weak repulsive interactions can hybridize the chiral ZLLs and a CSB gap $(\Delta)$ opens up at the double-Weyl points. The ZLLs are then placed at $\pm\sqrt{v^2k_z^2+\Delta^2}$.

The effective Hamiltonian for triple-WSMs reads as

$$H_3[\vec{A}] = i\gamma_0\left[\gamma_1\frac{\pi_+^3+\pi_-^3}{\Gamma}+\gamma_2\frac{\pi_+^3-\pi_-^3}{\Gamma}+\gamma_3 v k_z\right], \tag{16}$$

in a magnetic field $\vec{B} = B\hat{z}$, where the parameter $\Gamma$ controls the curvature of the cubic dispersion, and $\pi_\pm = \pi_x \pm i\pi_y$. The spectrum of LLs is given by $\pm\sqrt{\frac{l_B^{-6}}{\Gamma^2}n(n-1)(n-2)+v^2k_z^2}$. Hence, the chiral ZLL in a triple-WSM carries a threefold orbital degeneracy (for $n = 0,1,2$). Thus, sufficiently weak repulsive interactions can hybridize the chiral ZLL and open a spectral gap at the triple-Weyl points. The additional two- and three-fold degeneracies of the ZLLs, respectively, in double- and triple-WSMs stem from the bulk topological invariant of these two systems. Due to this additional degeneracy of the one-dimensional chiral ZLL, we expect the transition temperature for axionic CDW order in these materials to be higher than that in WSMs (neglecting the effect of disorder).

Note that the ZLLs in double- and triple-WSMs can also be gapped out by the SDW order. However, in these systems as well, the SDW order splits the filled LLs. Hence, we expect that even in double- and triple-WSMs, the CDW order is energetically favored over the SDW order.

## VI. AXIONIC DENSITY-WAVE, CHIRAL ANOMALY, AND TOPOLOGICAL DEFECTS

Momentum-space separation of Weyl nodes gives rise to a translational-symmetry-breaking CDW order in various members of the Weyl family at weak coupling in the presence of magnetic fields, which enters Eq. (2) as a complex mass $\Delta = m_1 + im_2$, and the U(1) angle $(\phi)$ between $m_1$ and $m_2$ is a dynamic variable. Thus, CDW order in WSMs represents an axionic state of matter, proposed several decades ago in the context of high-energy physics [55–57] and, more recently,

for paired ground states with $p+is$ symmetry in various three-dimensional doped narrow-gap semiconductors, such as $Cu_xBi_2Se_3$ and $Sn_{1-x}In_xTe$ [58] and a parity and time-reversal odd Kondo singlet order in a strongly correlated topological Kondo insulators [59]. However, experimental detection of axions has remained elusive. In this paper, we have shown that the axionic phase can be realized in various condensed matter systems at low $T$, such as DSMs (with Zeeman coupling) and WSMs, but, for weak repulsive interactions, when these systems are placed in strong magnetic fields.

The complex axionic mass can be represented as $m(\mathbf{r}) = |\Delta(\mathbf{r})|\ \exp[-i\mathbf{Q}\cdot\mathbf{r} - i\phi(\mathbf{r})]$, where $\mathbf{Q}$ is the separation of Weyl nodes in the BZ. After a local chiral transformation on the fermion field $\Psi(\mathbf{r}) \to \Psi(\mathbf{r})\exp[i(\mathbf{Q}\cdot\mathbf{r}+\phi(\mathbf{r}))\gamma_5/2]$ the complex mass becomes *real*. However, the path integral measure and the action are not invariant under such chiral transformation [60] and result in an anomalous magnetoelectric term,

$$\begin{aligned}\mathcal{S}_{\rm ax} &= n\times\frac{e^2}{32\pi^2}\int dtd\mathbf{r}\epsilon^{\mu\nu\rho\lambda}[\mathbf{Q}\cdot\mathbf{r}+\phi(\mathbf{r})]F_{\mu\nu}F_{\rho\lambda},\\ &= n\times\frac{e^2}{4\pi^2}\int dtd\mathbf{r}[\mathbf{Q}\cdot\mathbf{r}+\phi(\mathbf{r})]\mathbf{E}\cdot\mathbf{B},\end{aligned} \tag{17}$$

where $F_{\mu\nu}$ is the electromagnetic field strength tensor. The coefficient of the magnetoelectric term $n=1$, 2, and 3, respectively, for a WSM, double-WSM, and triple-WSM.

When a constant magnetic field is applied along the $z$ direction, the corresponding charge density is given by

$$j_0 = \frac{ne^2}{4\pi^2}(q_z+\partial_z\phi)B. \tag{18}$$

The first term gives rise to a layer quantum Hall effect with thickness $2n\pi/q_z$ accounting for the contribution from one-dimensional chiral surface states, residing at the boundary of WSMs, which can be observed in ARPES experiments. The second term is new and arises from the contribution of scattered states bound to the bulk of a WSM, the gapped ZLLs. Decomposing this term as $\frac{neB}{2\pi}\times\frac{e}{2\pi}\partial_z\phi$, we find that the second term corresponds to the one-dimensional charge density, while the first one accounts for the degeneracy of ZLLs in WSMs ($n=1$), double-WSMs ($n=2$), and triple-WSMs ($n=3$). The effect of this term appears only where $\partial_z\phi$ jumps, i.e., at the interface of WSMs with a vacuum. Hence, the bulk anomalous term $\mathcal{S}_{\rm ax}$ gives rise to surface Hall conductivity in WSMs, and through bulk-boundary correspondence the theory remains anomaly-free. Therefore, by comparing the separation of Weyl nodes from the ARPES measurements and the surface Hall conductivity, one can extract the contribution from the second term in $\mathcal{S}_{\rm ax}$ arising from bulk axionic CDW order.

So far, we have discussed the effect of the axionic density wave in the uniform phase. The U(1) CDW order can also allow the existence of topological defects, e.g., a *line vortex* or *axion string*, along the $z$ direction. For simplicity we consider the vorticity to be *one* and restrict ourselves to the *dilute* vortex limit. The line vortex accommodates $n$ number of chiral one-dimensional dispersive gapless fermionic modes in its core that carry a nondissipative electric current in the $z$ direction, determined by the one-dimensional chiral anomaly

$$j_z = n\times\frac{e^2E_z}{2\pi}, \tag{19}$$

with $n=1$, 2, and 3, respectively, for the WSM, double-WSM, and triple-WSM [61]. This current in turn is pumped from the bulk radially, which is captured by the bulk axionic term $\mathcal{S}_{\rm ax}$, according to the Callan-Harvey mechanism [32,62]. The exact solution of the dispersive modes can readily be obtained upon multiplying solutions of precise zero-energy modes bound to a *point vortex* in the $x$-$y$ plane [63] by the plane-wave factor $\exp(ik_zz)$. The existence of such one-dimensional gapless dispersive modes will manifest in a $T$-linear specific heat in the ordered phase when it accommodates a line vortex, which is distinct from $T^3$ dependence of the specific heat in the normal phase of three-dimensional WSMs.

## VII. SUMMARY AND CONCLUSIONS

To summarize, we here propose that both DSMs and WSMs can undergo a weak-coupling instability towards the formation of a CDW order in the presence of a strong magnetic field. Due to separation of Weyl nodes, which occurs naturally in WSMs, and due to Zeeman coupling in trivial as well as topological DSMs, the CDW order spontaneously breaks the translational symmetry and represents an axionic phase of matter. In this work, we demonstrate the effect of such mass generation on the renormalization of the charge and DMS and also analyze the scaling behavior of the spectral gap with the strength of the subcritical interactions and magnetic field. A similar mechanism has been argued to be operative in double- and triple-WSMs, where, due to the additional degeneracy of the ZLL, a larger gap can possibly be realized. Furthermore, we have argued that, between the CDW and the SDW orders, both of which can lead to a spectral gap at the Weyl points, the former one wins energetically since it pushes the filled LLs down in energy. Thus our proposed axionic phase of matter can be realized in topological DSMs, such as $Cd_2As_3$ [27] and $Na_3Bi$ [28], in recently found WSMs in TaAs [33–35], NbAs [36], TaP [37], $YbMnBi_2$ [38], and $Sr_{1-y}MnSb_2$ [39], and in various three-dimensional strong-spin-orbit-coupled materials, such as $Bi_2Se_3$, when these systems are placed in the close vicinity of the quantum critical point between the topological and the normal insulating phases. In addition, proposals for realizing double-WSMs in $HgCr_2Se_4$ [40–42] and $SrSi_2$ [43] give genuine hope that axionic CDW orders, corrections to DMS, and anomalous transport behavior can be observed in various members of the Weyl family in the near-future.

Besides the uniform ground state, we have also considered the role of topological defects in the ordered phase. Due to the associated U(1) angle in the axionic-CDW phase, the ordered state can support a line vortex, also known as an axion string. In the dilute vortex limit, we show that such a defect hosts $n$ number of one-dimensional gapless propagating modes, localized in its core, where $n=1$, 2, and 3 for the WSM, double-WSM, and triple-WSM, respectively when the vorticity in one. Thus the number of gapless modes is intimately tied to the topological invariant of the system. Such dispersive modes carries a nondissipative electric current

which in turn is supplied radially from the bulk, through the Callan-Harvey mechanism.

As a final remark, we comment on the role of disorder. Note that axionic CDW in the WSM, double-WSM, and triple-WSM breaks the translational symmetry due to momentum-space separation of the Weyl nodes. Most likely, the periodicity of such CDW order is incommensurate with the lattice periodicity. Therefore, axionic CDW can be susceptible to generic *disorders* [64], which may reduce the ordering temperature considerably. Nevertheless, we expect that in sufficiently clean systems and strong magnetic fields, a sizable mass gap can be observed in WSMs at low temperature.


## ACKNOWLEDGMENTS

B.R. is thankful to P. Goswami, P. Armitage, and N. Nagaosa for many fruitful discussions. We thank V. Juričić for critical reading of the manuscript. This work was supported by the startup grant to J.D.S. from the University of Maryland.


## APPENDIX: DERIVATION OF THE GAP EQUATION

We devote this Appendix to derive the gap equation, quoted in Eq. (13). The condensation energy in the presence of a CSB mass is given by

$$E = \frac{\Delta^2}{4g} - \frac{B}{2\pi}\int_{-\infty}^{\infty}\frac{dk_z}{2\pi}\left[\sqrt{\Delta^2+k_z^2} + 2\sum_{n\geqslant 1}\sqrt{2nB+k_z^2+\Delta^2}\right], \tag{A1}$$

as shown in Eq. (11). Minimizing $E$ with respect to $\Delta$ we obtain the gap equation

$$\begin{aligned}\frac{1}{g} &= \frac{B}{\pi}\int_{-\infty}^{\infty}\frac{dk_z}{2\pi}\left[\frac{1}{\sqrt{\Delta^2+k_z^2}} + \sum_{n\geqslant 1}\frac{2}{\sqrt{2nB+\Delta^2+k_z^2}}\right] = \frac{B}{\pi^{3/2}}\int_{\Lambda^{-2}}^{\infty}\frac{ds}{\sqrt{s}}\int_{-\infty}^{\infty}\frac{dk_z}{2\pi}e^{-s(k_z^2+\Delta^2)}\left[1+2\sum_{n\geqslant 1}e^{-s(2nB)}\right]\\ &= \frac{B}{\pi^2}\int_{\Lambda^{-2}}^{\infty}\frac{ds}{s}\left[-\frac{1}{2}+\sum_{n\geqslant 0}e^{-s(2nB)}\right]e^{-s\Delta^2} = \frac{B}{\pi^2}\int_{\Lambda^{-2}}^{\infty}\frac{ds}{s}\left[\frac{e^{2sB}}{e^{2sB}-1}-\frac{1}{2}\right]e^{-s\Delta^2} = \frac{B}{2\pi^2}\int_{\Lambda^{-2}}^{\infty}\frac{ds}{s}e^{-s\Delta^2}\coth(sB).\end{aligned} \tag{A2}$$

The above gap equation shows the UV divergence as we take the UV cutoff $\Lambda\to\infty$. To regulate this divergence (after taking $2\pi^2/g\to 1/g$), we can rewrite the gap equation as

$$\frac{1}{g} - \Lambda^2\int_0^{\infty}ds\frac{K(s)}{s^2} = -\int_{\Lambda^{-2}}^{\infty}\frac{ds}{s^2}[1-Bse^{-s\Delta^2}\coth(sB)], \tag{A3}$$

where the function $K(s)$ satisfies the asymptotic properties $K(s\to 0)=0$ and $K(s\to\infty)=1$, otherwise arbitrary. In terms of dimensionless variables $\Delta/(\Lambda v)\to m$ and $B/\Lambda^2\to B$, where $m,B\ll 1$, the above gap equation reduces to

$$\delta + I_1(m,B) + I_2(m,B) = 0, \tag{A4}$$

as shown in Eq. (13). For weak interactions $y = B/m^2 \gg 1$, and expanding the functions $I_1(m,B)$ and $I_2(m,B)$ for small $m$ and $B$, as well as large $y$, we obtain

$$I_2(m,B) = -B\int_1^{\infty}\frac{ds}{s}e^{-s\,m^2} = B\left[\gamma_E + 2\log(m) - m^2 + \frac{m^4}{4} + \mathcal{O}(m^6)\right], \tag{A5}$$

$$\begin{aligned}I_1(m,B) &= 2B\int_{2B}^{\infty}\frac{ds}{s^2}\left[1-\frac{se^{-s/(2y)}}{e^t-1}\right] = 2B\left[\int_0^{\infty}\frac{ds}{s^2}\left(1-\frac{s+\frac{1}{2}s^2}{e^s-1}\right)+\frac{1}{2}\left(1+\frac{1}{y}\right)\int_{2B}^{\infty}ds\left(\frac{1}{e^s-1}\right)\right.\\ &\left.-\frac{1}{2}\cdot\frac{1}{(2y)^2}\int_0^{\infty}ds\left(\frac{s}{e^s-1}\right)+\frac{1}{6}\cdot\frac{1}{(2y)^3}\int_0^{\infty}ds\left(\frac{s^2}{e^s-1}\right)-\mathcal{O}(y^{-4})\right]\\ &= 2B\left[0.63-\frac{0.21}{y^2}+\frac{0.05}{y^3}+\frac{1}{2}\left(1+\frac{1}{y}\right)\left\{-\log(2B)+B-\frac{B^2}{6}\right\}+\mathcal{O}(y^{-4},B^6)\right],\end{aligned} \tag{A6}$$

as shown in Eq. (14), and where

$$\delta = \frac{1}{g\Lambda^2} - \int_0^{\infty}ds\frac{K(s)}{s^2} \equiv \frac{1}{g\Lambda^2} - \frac{1}{\Lambda^2 g_c}, \quad \text{and} \quad \frac{1}{g_c} = \Lambda^2\int_0^{\infty}ds\frac{K(s)}{s^2}$$

is the zero-magnetic-field critical strength of the interaction for CSB ordering. Therefore, $\delta$ measures the deviation from the zero-magnetic-field critical point ($\delta=0$) and $\delta>0$ corresponds to a subcritical interaction, i.e., $g<g_c$.

[1] G. E. Volovik, *The Universe in a Helium Droplet* (Oxford University Press, New York, 2003).
[2] M. Z. Hassan and C. L. Kane, Rev. Mod. Phys. **82**, 3045 (2010).
[3] X. L. Qi and S.-C. Zhang, Rev. Mod. Phys. **83**, 1057 (2011).
[4] S.-Y. Xu, Y. Xia, L. A. Wray, S. Jia, F. Meier, J. H. Dil, J. Osterwalder, B. Slomski, A. Bansil, H. Lin, R. J. Cava, and M. Z. Hasan, Science **332**, 560 (2011).
[5] T. Sato, K. Segawa, K. Kosaka, S. Souma, K. Nakayama, K. Eto, T. Minami, Y. Ando, and T. Takahashi, Nat. Phys. **7**, 840 (2011).
[6] M. Brahlek, N. Bansal, N. Koirala, S.-Y. Xu, M. Neupane, C. Liu, M. Z. Hasan, and S. Oh, Phys. Rev. Lett. **109**, 186403 (2012).
[7] L. Wu, M. Brahlek, R. V. Aguilar, A. V. Stier, C. M. Morris, Y. Lubashevsky, L. S. Bilbro, N. Bansal, S. Oh, and N. P. Armitage, Nat. Phys. **9**, 410 (2013).
[8] X. Xi, C. Ma, Z. Liu, Z. Chen, W. Ku, H. Berger, C. Martin, D. B. Tanner, and G. L. Carr, Phys. Rev. Lett. **111**, 155701 (2013).
[9] H. B. Nielsen and M. Ninomiya, Phys. Lett. B **130**, 389 (1983).
[10] A. A. Burkov and L. Balents, Phys. Rev. Lett. **107**, 127205 (2011); A. A. Burkov, M. D. Hook, and L. Balents, Phys. Rev. B **84**, 235126 (2011).
[11] K. Y. Yang, Y. M. Lu, and Y. Ran, Phys. Rev. B **84**, 075129 (2011).
[12] A. A. Zyuzin, S. Wu, and A. A. Burkov, Phys. Rev. B **85**, 165110 (2012).
[13] V. Aji, Phys. Rev. B **85**, 241101 (2012).
[14] A. G. Grushin, Phys. Rev. D **86**, 045001 (2012).
[15] D. T. Son and B. Z. Spivak, Phys. Rev. B **88**, 104412 (2013).
[16] P. Goswami and S. Tewari, Phys. Rev. B **88**, 245107 (2013).
[17] M. M. Vazifeh and M. Franz, Phys. Rev. Lett. **111**, 206802 (2013).
[18] S. A. Parameswaran, T. Grover, D. A. Abanin, D. A. Pesin, and A. Vishwanath, Phys. Rev. X **4**, 031035 (2014).
[19] I. F. Herbut, V. Juričić, and B. Roy, Phys. Rev. B **79**, 085116 (2009).
[20] H. Wei, S.-P. Chao, and V. Aji, Phys. Rev. Lett. **109**, 196403 (2012).
[21] J. Maciejko and R. Nandkishore, Phys. Rev. B **90**, 035126 (2014).
[22] V. P. Gusysnin, V. A. Miransky, and I. A. Shovkovy, Nucl. Phys. B **462**, 249 (1996).
[23] See also V. P. Gusynin, V. A. Miransky, and I. A. Shovkovy, Phys. Rev. Lett. **83**, 1291 (1999); Phys. Lett. B **349**, 477 (1995); Nucl. Phys. B **563**, 361 (1999); D. M. Gitman, S. D. Odintsov, and Y. I. Shil'nov, Phys. Rev. D **54**, 2968 (1996).
[24] V. M. Yakovenko, Phys. Rev. B **47**, 8851 (1993).
[25] Z. Wang and S.-C. Zhang, Phys. Rev. B **87**, 161107(R) (2013).
[26] T. Morimoto and A. Furusaki, Phys. Rev. B **89**, 235127 (2014).
[27] S. Borisenko, Q. Gibson, D. Evtushinsky, V. Zabolotnyy, B. Büchner, and R. J. Cava, Phys. Rev. Lett. **113**, 027603 (2014).
[28] Z. K. Liu, B. Zhou, Z. J. Wang, H. M. Weng, D. Prabhakaran, S.-K. Mo, Y. Zhang, Z. X. Shen, Z. Fang, X. Dai, Z. Hussain, and Y. L. Chen, Science **343**, 864 (2014).
[29] $Cd_3As_2$ and $Na_3$ Bi host two copies of DSMs around $\pm\vec{Q}_0$. Zeeman splitting separates left and right fermions near each point.
[30] X. Wan, A. M. Turner, A. Vishwanath, and S. Y. Savrasov, Phys. Rev. B **83**, 205101 (2011).
[31] G. Y. Chao, arXiv:1110.1939.
[32] C. X. Liu, P. Ye, and X. L. Qi, Phys. Rev. B **87**, 235306 (2013).
[33] C. Zhang, Z. Yuan, S. Xu, Z. Lin, B. Tong, M. Z. Hasan, J. Wang, C. Zhang, and S. Jia, arXiv:1502.00251.
[34] S.-Y. Xu, I. Belopolski, N. Alidoust, M. Neupane, C. Zhang, R. Sankar, S.-M. Huang, C.-C. Lee, G. Chang, B. Wang, G. Bian, H. Zheng, D. S. Sanchez, F. Chou, H. Lin, S. Jia, and M. Z. Hasan, Science **347**, 294 (2015).
[35] B. Q. Lv, H. M. Weng, B. B. Fu, X. P. Wang, H. Miao, J. Ma, P. Richard, X. C. Huang, L. X. Zhao, G. F. Chen, Z. Fang, X. Dai, T. Qian, and H. Ding, Phys. Rev. X **5**, 031013 (2015).
[36] S.-Y. Xu, N. Alidoust, I. Belopolski, C. Zhang, G. Bian, T.-R. Chang, H. Zheng, V. Strokov, D. S. Sanchez, G. Chang, Z. Yuan, D. Mou, Y. Wu, L. Huang, C.-C. Lee, S.-M. Huang, B. K. Wang, A. Bansil, H.-T. Jeng, T. Neupert, A. Kaminski, H. Lin, S. Jia, and M. Z. Hasan, arXiv:1504.01350.
[37] N. Xu, H. M. Weng, B. Q. Lv, C. Matt, J. Park, F. Bisti, V. N. Strocov, D. Gawryluk, E. Pomjakushina, K. Conder, N. C. Plumb, M. Radovic, G. Autes, O. V. Yazyev, Z. Fang, X. Dai, G. Aeppli, T. Qian, J. Mesot, H. Ding, and M. Shi, arXiv:1507.03983.
[38] S. Borisenko, D. Evtushinsky, Q. Gibson, A. Yaresko, T. Kim, M. N. Ali, B. Buechner, M. Hoesch, and R. J. Cava, arXiv:1507.04847.
[39] J. Y. Liu, J. Hu, D. Graf, S. M. A. Radmanesh, D. J. Adams, Y. L. Zhu, G. F. Chen, X. Liu, J. Wei, I. Chiorescu, L. Spinu, and Z. Q. Mao, arXiv:1507.07978.
[40] G. Xu, H. Weng, Z. Wang, X. Dai, and Z. Fang, Phys. Rev. Lett. **107**, 186806 (2011).
[41] C. Fang, M. J. Gilbert, X. Dai, and B. A. Bernevig, Phys. Rev. Lett. **108**, 266802 (2012).
[42] B.-J. Yang, and N. Nagaosa, Nature Commun. **5**, 4898 (2014).
[43] S.-M. Huang, S.-Y. Xu, I. Belopolski, C.-C. Lee, G. Chang, B. K. Wang, N. Alidoust, M. Neupane, H. Zheng, D. Sanchez, A. Bansil, G. Bian, H. Lin, and M. Z. Hasan, arXiv:1503.05868.
[44] Y. Nambu and G. Jona-Lasinio, Phys. Rev. **122**, 345 (1961).
[45] E. V. Gorbar, V. A. Miransky, and I. A. Shovkovy, Phys. Rev. B **88**, 165105 (2013).
[46] In a lattice, since $|Q_3| \leqslant \pi$, the free energy needs to be minimized for $Q_3$ with an underlying lattice potential. Any finite $Q_3$ changes the location of the Weyl nodes, however, without qualitatively affecting our results.
[47] Z. Wang, Y. Sun, X.-Q. Chen, C. Franchini, G. Xu, H. Weng, X. Dai, and Z. Fang, Phys. Rev. B **85**, 195320 (2012).
[48] A. Salam and J. Strathdee, Nucl. Phys. B **90**, 203 (1975).
[49] P. Goswami and S. Chakravarty, Phys. Rev. Lett. **107**, 196803 (2011).
[50] I. F. Herbut and B. Roy, Phys. Rev. B **77**, 245438 (2008); B. Roy, M. P. Kennett, S. Das Sarma, *ibid.* **90**, 201409(R) (2014).
[51] H. Isobe and N. Nagaosa, Phys. Rev. B **86**, 165127 (2012).
[52] B. Roy, J. D. Sau, and S. Das Sarma, Phys. Rev. B **89**, 165119 (2014).
[53] S. Jeon, B. B. Zhou, A. Gyenis, B. E. Feldman, I. Kimchi, A. C. Potter, Q. D. Gibson, R. J. Cava, A. Vishwanath, and A. Yazdani, Nature Mater. **13**, 851 (2014).
[54] B. Roy, Phys. Rev. B **89**, 201401(R) (2014).
[55] R. D. Peccei and H. R. Quinn, Phys. Rec. Lett. **38**, 1440 (1977).
[56] S. Weinberg, Phys. Rev. Lett. **40**, 223 (1978).
[57] F. Wilczek, Phys. Rev. Lett. **40**, 279 (1978).
[58] P. Goswami and B. Roy, Phys. Rev. B **90**, 041301(R) (2014).

[59] B. Roy, J. D. Sau, M. Dzero, and V. Galitski, Phys. Rev. B **90**, 155314 (2014).
[60] K. Fujikawa and S. Suzuki, *Path Integrals and Quantum Anomalies* (Oxford University Press, New York, 2004).
[61] For an analogous situation in a superconducting line vortex, see B. Roy and P. Goswami, Phys. Rev. B **89**, 144507 (2014).
[62] C. G. Callan and J. A. Harvey, Nucl. Phys. B **250**, 427 (1985).
[63] C.-K. Lu and I. F. Herbut, Phys. Rev. Lett. **108**, 266402 (2012); C.-K. Lu and B. Seradjeh, Phys. Rev. B **89**, 245448 (2014); B. Roy, *ibid.* **85**, 165453 (2012).
[64] Y. Imry and S.-K. Ma, Phys. Rev. Lett. **35**, 1399 (1975).